PHYSICAL REVIEW E VOLUME 55, NUMBER 4 APRIL 1997

Self-consistent phonon approaches for the hydrogen bond chain

Yong-li Zhang and Wei-Mou Zheng
Institute of Theoretical Physics, Academia Sinica, P.O. Box 100080, Beijing, China
and State Key Laboratory for Scientific and Engineering Computing, CAS P.O. Box 2719, Beijing 100080, China

(Received 11 December 1996)

The hydrogen bonded ammonia chain model is studied by means of the standard self-consistent phonon approach and two modified versions. The effective crystal constant, force constant, free energy, and ratio of the first-order free energy to the zero order as a function of temperature are numerically obtained with the three approaches, and then compared. The standard approach gives the lowest free energy. Violation of the convexity is found in one of the modified approaches near the temperature which is regarded as the melting temperature. [S1063-651X(97)06704-4]

PACS number(s): 87.15.By, 87.15.Kg, 63.70.+h

I. INTRODUCTION

Self-consistent phonon approaches (SCPAs) have been widely used in solid state physics to study the effects of anharmonic potentials on thermal conduction and expansion of solids [1,2] and structural phase transitions [3]. The conformation of biological macromolecules is, to a large extent, determined by hydrogen bonds, Coulomb interactions, and van der Waals interactions, which are weaker than chemical covalent bonds. Under these forces atoms or chemical groups in a macromolecule may undergo motions of a large amplitude at a physiological temperature, and anharmonic terms in potentials can make a significant contribution to the thermodynamic properties of the macromolecules, such as the specific heat of a crystalline protein. The SCPA then provides a useful tool. An example of the succsessful usage of SCPA in the field of biophysics is the calculation of normal modes for biological macromolecules including DNA molecules by Prohofsky and co-workers [4]. Compared with the conventional phonon perturbation theory, the SCPA has a larger scope of applicability. As verified in experiments of low frequency Raman scattering and inelastic neutron scattering, at a low temperature the chemical groups in a DNA molecule move with a relatively small amplitude. The vibrational modes of DNA molecules at low temperature and their shifts with temperature calculated by Prohofsky and co-workers agree with the spectral measurements of many spectral lines at low frequencies.

Efforts have been made to extend the method to the problem of DNA denaturation or melting [5]. As is well known in quantum crystal theory, the SCPA is inadequate to describe the melting of solids [6]. To overcome this limitation, Prohofsky and co-workers, introduced a new self-consistent displacement condition (SCDC) and proposed a modified self-consistent phonon approach (MSPA) [7]. Using the MSPA, they studied a simple model of the hydrogen bonded ammonia chain [8]. Although it is an imaginary system, hydrogen bond chains or rings do widely exist in nature, especially in biological systems. Examples are short-lived chains in water, organic solutions or hydrate crystals, and short structural water chains in enzymes [9,10]. There are also hydrogen bonding networks, for which the model may provide an approximation for a special dimension [10]. With this ammonia chain model we shall make a comparison between SCPA and MSPA.

The paper is organized as follows. In Sec. II we derive the conventional self-consistent condition for the force constant and displacement based on the Gibbs-Bogoliubov inequality, and give the self-consistent condition used in MSPA and the one used in Ref. [11]. In Sec. III some numerical comparison is made among the three kinds of self-consistent conditions. Finally, in Sec. IV we make a few concluding remarks. Some mathematical derivation is included in the Appendix.

II. THREE VERSIONS OF THE SELF-CONSISTENT PHONON APPROACH

In the ammonia chain model of Ref. [8], ammonia molecules are displaced along an axis on which two nitrogen atoms of neighboring amimonia molecules form an H bond described by the Morse potential

$$V(r)=V_0\{1-\exp[-a(r-R_0)]\}^2-V_0, \tag{1}$$

where $V_0=3.48$ kcal/mol, $R_0=3.37$ Å, and $a=1.22$ Å^{-1}. The Hamiltonian of the system is

$$H=\sum_n\left[\frac{p_n^2}{2M}+V(y_{n+1}-y_n)\right], \tag{2}$$

where M is the mass of the ammonia molecule, and y_n the position of the nth molecule. In order to make a self-consistent harmonic approximation, we consider a trial Hamiltonian

$$H_0=\sum_n\left[\frac{p_n^2}{2M}+\frac{1}{2}\phi(x_n-x_{n-1})^2\right]-NV_0, \tag{3}$$

where x_n is the displacement of the nth molecule from its equilibrium position in the harmonic chain. Assuming the lattice constant for the harmonic chain described by H_0 to be R_T, which is to be fixed later, we relate x_n to y_n through

$$x_n-x_{n-1}+R_T=y_n-y_{n-1}. \tag{4}$$

The free energy F_0 of the trial system is

$$F_0=\beta^{-1}\sum_k \ln[2\sinh(\tfrac{1}{2}\beta\hbar\omega_k)]+NV_0. \tag{5}$$

According to the Gibbs-Bogoliubov inequality, the free energy F of the original system satisfies

$$F\leqslant F_1=F_0+\langle H-H_0\rangle_0, \tag{6}$$

where we have used the notation

$$\langle\theta\rangle_0\equiv\frac{\mathrm{Tr}[\theta\exp(-\beta H_0)]}{\mathrm{Tr}[\exp(-\beta H_0)]}.$$

In fact, F_1, giving the upper bound of the actual free energy F, is the first order of the cumulative expansion of F with respect to the trial system. The lower the free energy F_1, the closer is the trial system to the real one. So minimizing F_1 optimizes the approximation. Moreover, the inequality can also be taken as a validity criterion for different approximate trial Hamiltonians. Minimizing F_1 with respect to its two parameters ϕ and R_T, we have

$$\frac{\partial F_1}{\partial\phi}=0, \tag{7}$$

$$\frac{\partial F_1}{\partial R_T}=0, \tag{8}$$

which are the self-consistent conditions for the force constant ϕ and displacement R_T. Taking advantage of the harmonic system, we can calculate

$$\langle H-H_0\rangle_0=N\langle V(y_2-y_1)\rangle_0-N\phi D/2, \tag{9}$$

where the correlation function D is defined as

$$D=\langle(x_2-x_1)^2\rangle_0. \tag{10}$$

Using the formulas derived in the Appendix, we have

$$D=\frac{2\hbar}{NM}\sum_k \omega_k^{-1}\coth(\tfrac{1}{2}\beta\hbar\omega_k)\sin^2(\tfrac{1}{2}kR_T), \tag{11}$$

$$\langle V(y_2-y_1)\rangle_0=\exp\left(\frac{D}{2}\frac{\partial^2}{\partial\xi^2}\right)V(\xi)\bigg|_{\xi=R_T}\equiv\exp(\tfrac{1}{2}D\partial_\xi^2)V(R_T). \tag{12}$$

As given in the Appendix, the dispersion relation of the one-dimensional (1D) harmonic system is

$$\omega_k^2=\frac{4\phi}{M}\sin^2(\tfrac{1}{2}kR_T). \tag{13}$$

From Eqs. (5) and (13) we have

$$\frac{\partial F_0}{\partial\phi}=\sum_k\frac{\partial F_0}{\partial\omega_k}\frac{\partial\omega_k}{\partial\phi}=\frac{1}{2}ND, \tag{14}$$

where Eq. (11) has been used in deriving the last equality. Thus, from the definition (6) of F_1 and Eqs. (7), (12), and (14), we find

$$\frac{\partial F_1}{\partial\phi}=\frac{N}{2}\frac{\partial D}{\partial\phi}[\exp(\tfrac{1}{2}D\partial_\xi^2)V''(R_T)-\phi]=0, \tag{15}$$

or

$$\phi=\exp(\tfrac{1}{2}D\partial_\xi^2)V''(R_T). \tag{16}$$

The Hamiltonain H_0 is independent of R_T, so F_0 would be also. Under the periodic boundary condition $kR_T=-\pi+2\pi n/N,\ n=1,2,\ldots,N$. A direct estimation of F_0 from Eq. (5) will also show its independence of R_T, i.e., $\partial F_0/\partial R_T=0$. From Eqs. (8) and (12) we find

$$\frac{\partial F_1}{\partial R_T}=N\exp\left(\frac{D}{2}\frac{\partial^2}{\partial\xi^2}\right)V'(R_T)=0. \tag{17}$$

Equations (16) and (17) are self-consistent conditions to determine the trial harmonic Hamiltonian. Using a Fourier transformation, we may express them as

$$\begin{aligned}\phi&=\frac{1}{2\pi}\int dq\exp\left(-\frac{D}{2}q^2\right)\int duV''(R_T+u)e^{iqu}\\&\approx\int_{\varepsilon-R_T}^{+\infty}du\exp\left(-\frac{u^2}{2D}\right)V''(R_T+u)\bigg/\int_{\varepsilon-R_T}^{+\infty}du\\&\quad\times\exp\left(-\frac{u^2}{2D}\right),\end{aligned} \tag{18}$$

$$\int du\exp\left(-\frac{u^2}{2D}\right)V'(R_T+u)=0, \tag{19}$$

where ε is the truncation parameter for a hard core. The two conditions (18) and (19) have the physical meaning that the effective force constant is not the local force constant at the potential minimum, but the thermodynamical average of force constants, and the equilibrium position is determined by averaging force. That is, $\phi=\langle V''(R_T)\rangle_0$, and $\langle V'(R_T)\rangle_0=0$. They are coupled with each other, and must be solved self-consistently.

In the MSPA, the equilibrium position is instead determined by

$$V[R_T+\mu(T)]=V[R_T-\mu(T)], \tag{20}$$

where $\mu(T)$ is the half-width of the weight function $\exp(-u^2/2D)$, i.e., $\exp(-\mu^2/2D)=1/2$, and is regarded as a classical oscillatory amplitude. In this way, the equilibrium position is taken at the midpoint of two classical turnaround points fixed by μ [7].

In Ref. [11], discussing the dissociation of a hydrogen bound in a dimer molecule, such as an ammonia dimer based on SCPA, Galindo and Sokoloff employed another different self-consistent condition for the equilibrium position, i.e.,

$$\frac{d}{dR_T}\langle V(R_T)\rangle_0=0. \tag{21}$$

This version of SCPA shall be referred to as the revised self-consistent phonon approach (RSPA). The previous condition (19) implies that

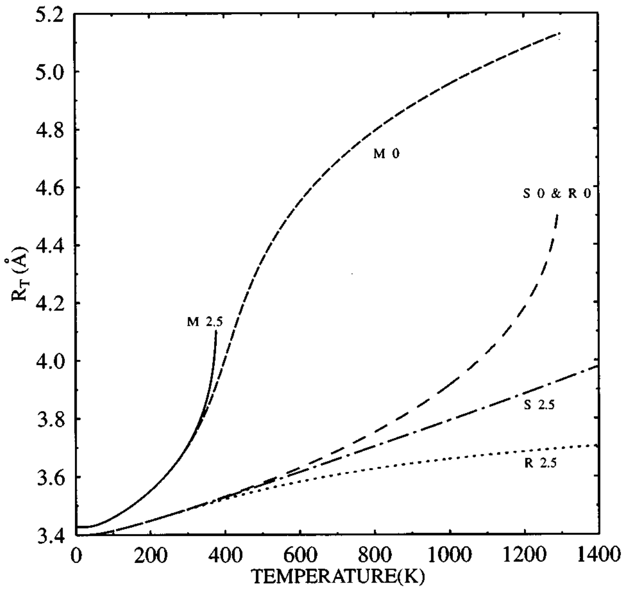

FIG. 1. Dependence of the effective chain crystal constant R_T on temperature. Curves are labeled by "*S*," "*M*," and "*R*" for SCPA, MSPA and RSPA, and by numbers "2.5" and "0" for the corresponding cases with and without a hard core of $\varepsilon = 2.5$ Å, respectively.

$$\frac{d}{dR_T}\int_{\varepsilon-R_T}^{+\infty} du \exp\left(-\frac{u^2}{2D}\right) V(R_T+u) = \exp\left(-\frac{(\varepsilon-R_T)^2}{2D}\right) V(\varepsilon) \equiv \delta(\varepsilon). \tag{22}$$

When $|\varepsilon - R_T| \gg D$, e.g., for the case without a hard core, $\delta(\varepsilon) \approx 0$. The difference between SCPA and RSPA is very small.

In Sec. III we shall compare these three kinds of self-consistent conditions numerically.

III. NUMERICAL COMPARISON

As in Refs. [8] and [11], the Einstein approximation for the phonon spectrum is also adopted in our calculation. Although the Morse potential already includes some hard core effect [12], a hard core ε was set in Refs. [8] and [11]. In order to make a better comparison, we consider both cases with, as well as without, a hard core. In Ref. [8] no hard core ε was explicitly given, while in Ref. [11] a hard core of $\varepsilon = 2.8$ Å was chosen. To reproduce results similar to the references we set $\varepsilon = 2.5$ Å. Results corresponding to the three different equilibrium position conditions (19), (20), and (21) are marked with "*S*," "*M*," and "*R*," respectively. Numbers "0" and "2.5" are used to distinguish the case without a hard core from that with a hard core.

(i) Thermal expansion. The effective crystal constant R_T as a function of the temperature T is plotted in Fig. 1. A sharp growth of R_T is found for MSPA with $\varepsilon = 2.5$ Å, indicating a "reasonable" melting temperature around 377 K. When the temperature is higher than 377 K, no self-consistent solution exists for MSPA. For SCPA and RSPA with $\varepsilon = 0$ a comparable sharp growth in R_T is seen at a temperature near 1300 K, which is much higher than 377 K. For $\varepsilon = 2.5$ Å both SCPA and RSPA show that the system just undergoes a linear thermal expansion with increasing temperature, and no melting happens in the temperature region considered.

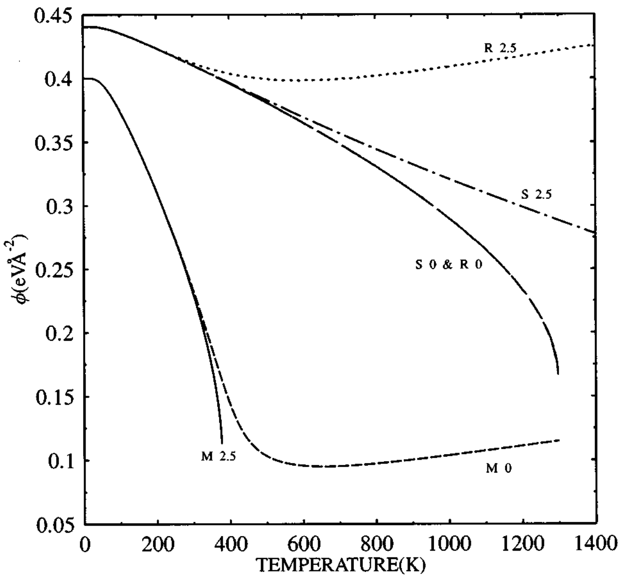

FIG. 2. Effective force constant as a function of temperature.

As discussed in Sec. II, for $\varepsilon = 0$ RSPA almost coincides with SCPA. Taking typical values $R_T = 4.0$ Å and $D = 0.4$ Å^2, we have estimated $\delta(0) \approx 10^{-9}$ and $\delta(2.5) \approx 0.02$. This explains the difference between SCPA and RSPA seen at $\varepsilon = 2.5$ Å. At a very low temperature, D is rather small, so the difference is also significantly reduced.

(ii) Effective force constant. In Fig. 2 we plot the effective force constant ϕ as a function of the temperature T. As far as melting is concerned, Figs. 1 and 2 are consistent. At the melting temperature a sharp drop in ϕ is seen. Generally, the MSPA harmonic chain is much softer than the other two. Furthermore, both MSPA and RSPA show an unreasonable growth of ϕ with increasing temperature at $T > 500$ K for $\varepsilon = 2.5$ Å.

(iii) Free energy. The free energy F_1 as a function of T is shown in Fig. 3. In the low temperature region (0–200 K), three approaches give approximately the same free energy for both hard core parameters. When the temperature increases, the discrepancy among the three approaches becomes prominent. The MSPA gives a free energy much higher than those of SCPA and RSPA, and the SCPA always gives the lowest free energy. If we regard the Gibbs-Bogoliubov inequality as a criterion for the validity of approximation, the MSPA is the poorest. Moreover, near the MSPA melting temperature the MSPA free energy for both $\varepsilon = 0$ and 2.5 Å violates the convexity condition, exhibiting an unphysical negative special heat.

(iv) Ratio of $\langle H - H_0 \rangle_0$ to F_0. Regarding F_1 as the first-order cumulant expansion, we plot the ratio $\langle H - H_0 \rangle_0 / F_0$ as a function of T in Fig. 4. In a wide temperature region the absolute value of this ratio is within 0.05 for SCPA and RSPA. On the contrary, the ratio is beyond 0.2 near the MSPA melting temperature 377 K. Higher-order terms should be very important for MSPA.

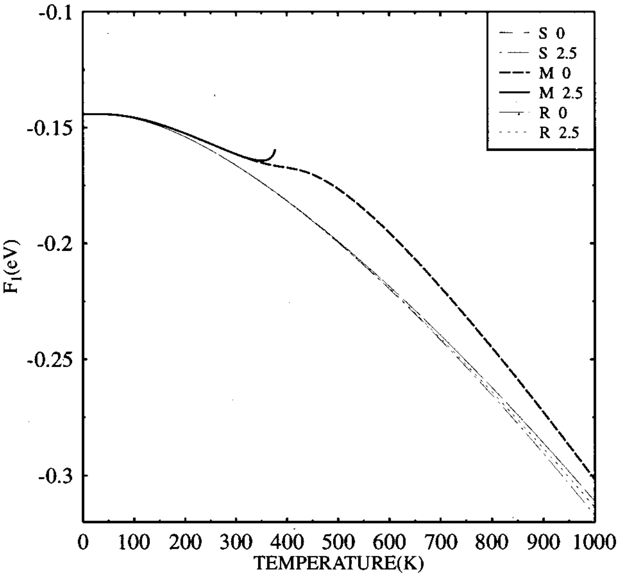

FIG. 3. Comparison of free energy as a function of temperature. Curves from top, in succession, are MSPA with $\varepsilon=2.5$, MSPA with $\varepsilon=0$, overlapping curve of SCPA and RSPA with $\varepsilon=0$, RSPA with $\varepsilon=2.5$ and SCPA with $\varepsilon=2.5$, respectively.

IV. CONCLUSION

We have compared three self-consistent phonon approaches: SCPA, MSPA, and RSPA, which differ from each other in the condition for the effective crystal constant. At low temperature the three approaches give almost the same result. The SCPA and RSPA, giving a very high temperature for a rapid lattice softening, are inadequate for describing melting. Although MSPA is able to provide a reasonable melting temperature, the approach itself, violating the convexity condition for free energy near this melting temperature, is not valid for that temperature region. To describe the phenomenon of melting new approaches have to be developed.

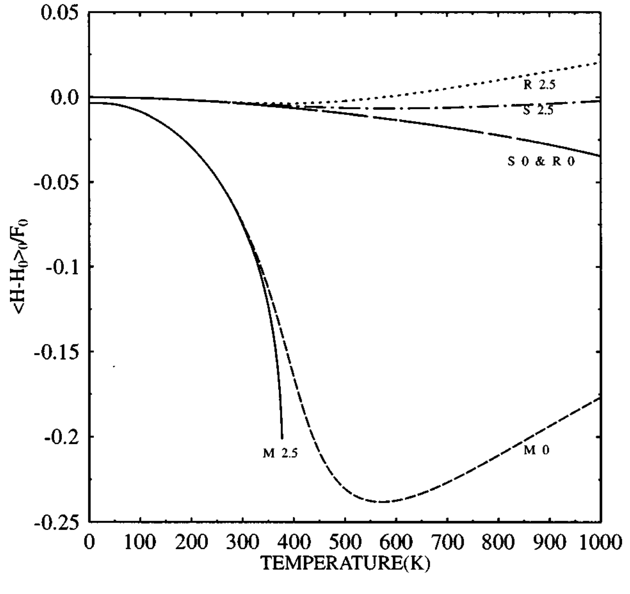

FIG. 4. Dependence of the ratio $\langle H-H_0\rangle_0/F_0$ on temperature.

ACKNOWLEDGMENTS

The authors thank Bai-lin Hao and Yu-zong Chen for valuable discussions. This work was supported in part by the National Natural Science Foundation of China.

APPENDIX

According to the theory of lattice dynamics [13], we represent x_m and p_m as

$$x_m=\sum_k \left(\frac{\hbar}{2NM\omega_k}\right)^{1/2}(a_k^\dagger e^{-imkR}+a_k e^{imkR}),$$

$$p_m=\sum_k i\left(\frac{\hbar M\omega_k}{2N}\right)^{1/2}(a_k^\dagger e^{-imkR}-a_k e^{imkR}), \qquad (A1)$$

where we have denoted the lattice constant by R instead of R_T. Substituting Eq. (A1) into the Hamiltonian (3) and dropping the trival term NV_0, we find

$$H_0=\sum_k \frac{1}{2}\hbar\omega_k(a_k^\dagger a_k+\tfrac{1}{2})+\sum_k \frac{2\hbar\phi}{M\omega_k}\sin^2(\tfrac{1}{2}kR)(a_k^\dagger a_k+\tfrac{1}{2})$$

$$\equiv\sum_k \hbar\omega_k(a_k^\dagger a_k+\tfrac{1}{2}), \qquad (A2)$$

where in writing the last equality we have deduced the dispersion relation (13).

Defining

$$d_k=\left(\frac{\hbar}{2NM\omega_k}\right)^{1/2}(e^{-imkR}-e^{-inkR}), \qquad (A3)$$

we have

$$x_{mn}=x_m-x_n=\sum_k (d_k^* a_k+d_k a_k^\dagger). \qquad (A4)$$

Thus,

$$D_{mn}\equiv\langle x_{mn}^2\rangle_0$$

$$=\sum_k \sum_{l_k} |d_k|^2\langle l_k|(a_k a_k^\dagger+a_k^\dagger a_k)|l_k\rangle e^{-\beta(l_k+1/2)\hbar\omega_k}/Z_k$$

$$=\sum_k \frac{1+e^{-\beta\hbar\omega_k}}{1-e^{-\beta\hbar\omega_k}}|d_k|^2, \qquad (A5)$$

where Z_k is defined by

$$Z_k=\frac{e^{-(1/2)\beta\hbar\omega_k}}{1-e^{-\beta\hbar\omega_k}}. \qquad (A6)$$

From Eqs. (A3) and (A5), we obtain

$$D_{mn}=\frac{\hbar}{NM}\sum_k \frac{1}{\omega_k}\coth(\tfrac{1}{2}\beta\hbar\omega_k)\{1-\cos[(m-n)kR]\}. \qquad (A7)$$

By noticing $D=D_{21}$ Eq. (11) is verified.

Let us introduce

$$\gamma_k = d_k \frac{\partial}{\partial \xi} \equiv d_k \partial_\xi .$$

We then have

$$\begin{aligned}\langle \exp(x_{mn}\partial_\xi)\rangle_0 &= \left\langle \exp\left[\sum_k (\gamma_k^* a_k + \gamma_k a_k^\dagger)\right]\right\rangle_0 \\ &= \prod_k \langle \exp(\gamma_k^* a_k + \gamma_k a_k^\dagger)\rangle_0 ,\end{aligned} \tag{A8}$$

where

$$\begin{aligned}\langle \exp(\gamma_k^* a_k + \gamma_k a_k^\dagger)\rangle_0 &= \frac{1}{Z_k}\sum_{n_k=0}^{\infty} \langle n_k|\exp(\gamma_k a_k + \gamma_k^* a_k^\dagger)|n_k\rangle \\ &\quad \times e^{-\beta(n_k+1/2)\hbar\omega_k} .\end{aligned} \tag{A9}$$

Using the formulas

$$e^{\gamma^* a + \gamma a^\dagger} = e^{\gamma^* a} e^{\gamma a^\dagger} e^{(1/2)|\gamma|^2}, \tag{A10}$$

$$e^{\gamma a^\dagger}|n\rangle = \sum_{m=0}^{\infty} \frac{1}{m!}(\gamma)^m \left(\frac{(m+n)!}{n!}\right)^{1/2} |m+n\rangle, \tag{A11}$$

we obtain

$$\langle n|\exp(\gamma^* a + \gamma a^\dagger)|n\rangle = e^{-(1/2)|\gamma|^2} \sum_m |\gamma|^{2m} \frac{(m+n)!}{(m!)^2 n!} . \tag{A12}$$

By means of the binomial expansion

$$(1-x)^{-m-1} = \sum_{n=0}^{\infty} \frac{(m+n)!}{m!n!} x^n , \tag{A13}$$

from Eqs. (A12) and (A13) we have

$$\begin{aligned}\langle \exp(\gamma_k^* a_k + \gamma_k a_k^\dagger)\rangle_0 &= \exp\left[|\gamma_k|^2\left(-\frac{1}{2} + \frac{1}{1-e^{-\beta\hbar\omega_k}}\right)\right] \\ &= \exp[\tfrac{1}{2}\coth(\tfrac{1}{2}\beta\hbar\omega_k)|\gamma_k|^2].\end{aligned} \tag{A14}$$

Finally, we reduce Eq. (30) to

$$\begin{aligned}\langle \exp(x_{mn}\partial_\xi)\rangle_0 &= \exp\left[\tfrac{1}{2}\sum_k \coth(\tfrac{1}{2}\beta\hbar\omega_k)|\gamma_k|^2\right] \\ &= \exp(\tfrac{1}{2}D_{mn}\partial_\xi^2),\end{aligned} \tag{A15}$$

which is the same as Eq. (12) for $D = D_{21}$.

[1] W. Gotze, K. H. Michel, and T. R. Koehler, in *Dynamical Properties of Solids*, edited by G. K. Horton and A. A. Maradudin (North-Holland, Amsterdam, 1975), Vols. 1 and 2.

[2] N. S. Gilis and N. R. Werthamer, Phys. Rev. **165**, B951 (1968); N. R. Werthamer, Am. J. Phys. **37**, 763 (1969); N. R. Werthamer, Phys. Rev. B **1**, 572 (1970).

[3] J. R. Morris and R. J. Gooding, Phys. Rev. Lett. **65**, 1769 (1990).

[4] J. M. Eyster and E. W. Prohofsky, Biopolymers **13**, 2503 (1974); **13**, 2527 (1974); Y. Z. Chen and E. W. Prohofsky, *ibid.* **35**, 657 (1995).

[5] E. W. Prohofsky, *Statistical Mechanics and Stability of Macromolecules* (Cambridge University Press, Cambridge, England, 1995).

[6] V. V. Goldman, G. K. Horton, and M. L. Klein, Phys. Rev. Lett. **21**, 1527 (1968).

[7] Y. Gao, K. V. Devi-Prasad, and E. W. Prohofsky, J. Chem. Phys. **80**, 6291 (1984).

[8] Y. Gao and E. W. Prohofsky, J. Chem. Phys. **80**, 2242 (1984).

[9] L. Ojamae and K. Hermansson, J. Phys. Chem. **98**, 4271 (1994).

[10] G. A. Jeffrey and W. Saenger, *Hydrogen Bonding in Biological Structures* (Springer, Berlin, 1994).

[11] C. E. Galindo and J. B. Sokoloff, Phys. Rev. E **48**, 3091 (1993).

[12] P. M. Morse, Phys. Rev. **34**, 57 (1929).

[13] J. Callaway, *Quantum Theory of the Solid State* (Academic, New York, 1991).